AIMS Mathematics, 11(5): 14668–14692.
DOI: 10.3934/math.2026602
Received: 27 January 2026
Revised: 24 April 2026
Accepted: 11 May 2026
Published: 25 May 2026

https://www.aimspress.com/journal/Math

*Research article*

# Lyapunov-based stabilization control design of space 2-D linear parabolic distributed parameter systems employing mobile sensors and actuators

**Xiao-Wei Zhang, Xiang-Jie Pu, Xiaoli Li* and Zi-Peng Wang**

School of Information Science and Technology, Beijing University of Technology, Beijing 100124, China

* **Correspondence:** Email: lixiaolibjut@bjut.edu.cn.

**Abstract:** For the actual physical temporal-space process, the spatial two-dimensional (2-D) case makes more sense. With the increase of space dimension, the difficulty of control design increases sharply. This study investigates the asymptotic stabilization issue for 2-D linear parabolic distributed parameter systems (DPSs) defined over spatial domains, where the control architecture incorporates dynamically collocated sensors and actuators. First, in light of the number of mobile sensor/actuator pairs, the 2-D spatial domain is divided into the corresponding quantity of spatial subdomains. At the same time, the mobile sensor/actuator pairs are forced to move in their respective subdomains under the restriction of projection modification algorithm. Afterwards, based on operator semigroup theory, the well-posedness of open-loop and closed-loop spatial 2-D DPSs is both studied. Aiming at the stabilization control of spatial 2-D DPSs under mobile sensor/actuator pairs, we put forward an integrated design scheme of mobile sensor/actuator guidance and static output feedback controller to guarantee the asymptotic stability of the 2-D closed-loop system. Finally, it can be concluded from a simulation example that the proposed integrated design method is effective.

**Keywords:** space 2-D linear distributed parameter systems; static output feedback controller; sensor/actuator mobile guidance
**Mathematics Subject Classification:** 35K57, 93C20, 93D15

## 1. Introduction

Distributed parameter systems (DPSs), typically governed by partial differential equations (PDEs) [1–3], play a crucial role in numerous industrial and environmental applications, including chemical process control , metallurgical production optimization, and water resource quality regulation [4–6]. For the purpose of fully taking into account the system characteristics, plenty of design methodologies based on the original PDE model were developed for PDE systems. For

instance, the reference [7] introduced the Volterra integral transformation to provide a boundary control method for linear parabolic PDE systems. Along with this design idea, a large number of research results have emerged, such as adaptive boundary control [8], boundary stabilization control [9], output regulation boundary control [10, 11], and active disturbance rejection control [12]. Based on the finite-dimensional observer, the authors of [13] provided a control design method for linear delayed PDE systems. In [14], a novel spatio-temporal least squares support vector machine framework was developed to model complex nonlinear PDE systems, and the proposed methodology has been effectively implemented in real-world thermal curing processes with promising results. Furthermore, reference [15] introduced an adaptive Karhunen-Loève decomposition combined with fuzzy modeling to effectively capture the time-varying spatiotemporal dynamics inherent in thermal curing processes, demonstrating improved accuracy and flexibility. In [16], the authors designed a boundary controller of the flexible robotic manipulator to address input backlash. Recently, fuzzy logic-based control strategies, including fuzzy adaptive-event-triggered tracking control [17–19], fuzzy iterative learning control [20], and fuzzy proportional-integral-derivative boundary output tracking [21], have been widely investigated for nonlinear PDE systems. Additionally, the control design has been successfully extended to stochastic frameworks, addressing challenging issues such as the finite-time stabilization of impulsive stochastic DPSs [22, 23]. However, static sensors and actuators are employed to acquire the mentioned results above.

As users gradually realize the advantages of mobile sensors and actuators, the PDE system control with moving devices has received extensive attention [24–26]. Compared with static sensors and actuators, the mobile equipment can improve the control performance, reduce the risk of human operation, and lower the economic cost. Especially, Lyapunov stability theory has been widely used in control and guidance of PDE systems. For example, reference [27] proposed a combination control scheme to improve the performance of PDE systems via nonconfiguration mobile sensors and actuators. Reference [28] put forward a scheme of combining mobile guidance with feedback control, and optimized the guidance of the mobile actuators so that they can be in the specified area without explicit constraints. In [29], the radar obstacle avoidance technology was applied to time-delay PDE systems. To deal with the external disturbance, the authors of [30] introduced an $H_\infty$ performance constraint, and two design methods of feedback compensators were proposed with respect to collocated/noncollocated cases. In [31], the authors designed an appropriate switched sampled-data control method for the stabilization of the Kuramoto-Sivashinsky equation with spatially scheduled actuators and sensors, and the proposed switching controller was able to reduce the energy consumption. Moreover, an integrated design method combining control with mobile guidance was developed to render the closed-loop PDE system exponentially stable, and the designed mobile guidance laws can effectively improve the transient response of the closed-loop state [32–34]. In [32], the closed-loop stability of linear PDE systems using mobile sensors and actuators was achieved through an integrated design combining control strategies with motion coordination laws. In [33], the authors researched the $H_\infty$ control design problem of nonlinear PDE systems. Based on the integrated scheme of control and guidance, the closed-loop system not only satisfied the specified $H_\infty$ disturbance attenuation performance, but also ensured the exponential stability. Reference [34] studied the Lyapunov-based stabilization of a delayed linear parabolic PDE system under mobile sensors and actuators, and put forward a delay-dependent control plus guidance scheme. Recently, on the basis of the Takagi-Sugeno fuzzy model, references [35–37] have presented some control methods including

fuzzy controller and mobile device guidance, and these plentiful research results constructed the fuzzy DPS control theory based on moving sensors and actuators. However, the studies mentioned above were all aimed at spatial one-dimensional DPSs, and the spatial two-dimensional (2-D) situation is more meaningful for the actual physical spatiotemporal processes.

In recent years, increasing attention has been paid to the design of spatial 2-D parabolic DPSs [38–40]. In [41, 42], for the 2-D diffusion process of toxic substances, a practical algorithm via Centroidal Voronoi Tessellations (CVT) was proposed to resolve the movement planning problem of the mobile actuators, which extended the application of CVT to feedback control with mobile actuators. In [43,44], a coordinated optimization approach was developed for 2-D DPS regulation using mobile actuators, simultaneously solving the optimal control problem and actuator trajectory planning. In particular, reference [45] put forward an abstract framework for the optimization of sensing and executing devices in 2-D DPSs. On the basis of the process dynamic characteristic, a control scheme with mobile sensors and actuators was proposed to enhance the closed-loop performance, where the Lyapunov stability argument was utilized to provide a stable guidance scheme for each mobile device, and the designed guidance scheme was equally applicable to the state estimation issue under mobile sensors. The considered sensor/actuator pairs were mounted on a differential drive robotic platform [46] and governed by standard 2-D dynamics, where a gradient-driven navigation strategy was developed by utilizing the platform's torque control to steer the vehicle toward high-gradient regions of the spatial domain. However, stabilizing control synthesis for 2-D linear parabolic DPSs using mobile sensors and actuators still presents unresolved challenges in current research, which motivates the current work.

**Table 1.** Notations.

| Symbol | Description |
|---|---|
| $\mathbb{R}$ | The set of real numbers |
| $\mathbb{R}^n$ | $n$-dimensional Euclidean space |
| $W$ | $(0,\alpha)\times(0,\beta)$ |
| $\mathcal{L}^2(W)$ | A real Hilbert space of square integrable scalar functions $v(g,k): W\to\mathbb{R}$ with the inner product induced norm $\lvert v(\cdot,\cdot)\rvert_2 \triangleq \sqrt{\int_W v^2(g,k)dgdk}$ |
| $\mathcal{H}^2(W)$ | A real Sobolev space of absolutely continuous scalar functions $v(g,k): W\to\mathbb{R}$ with the square integrable derivative $\triangle v(g,k)$ and the norm $\lvert v(\cdot,\cdot)\rvert_{\mathcal{H}^2(W)} \triangleq \sqrt{\int_W (v^2+\nabla v^T\nabla v+(\Delta v)^2)dgdk}$ |
| leb($W$) | The Lebesgue measure of the domain $W$ |
| dia($W$) | The diameter of the domain $W$ |
| $\triangle v(g,k)$ | $\frac{\partial^2 v(g,k)}{\partial g^2}+\frac{\partial^2 v(g,k)}{\partial k^2}$ |
| $\nabla v(g,k)$ | $\left[\frac{\partial v(g,k)}{\partial g}\ \ \frac{\partial v(g,k)}{\partial k}\right]^T$ |

This article provides a comprehensive framework for the stabilization control of space 2-D linear parabolic DPSs using moving sensor/actuator pairs. The spatial domain is partitioned into multiple

nonoverlapping subdomains along both spatial dimensions, with each sensor/actuator pair constrained to move exclusively within its designated subdomain via a projection correction algorithm. A rigorous well-posedness analysis is conducted for both open-loop and closed-loop systems to establish their mathematical validity. Leveraging the Lyapunov direct method, we develop an integrated control and guidance synthesis of a 2-D DPS, formulated through linear matrix inequality (LMI) techniques to ensure the asymptotic stability of the closed-loop system. Numerical simulations validate the efficacy of the proposed control-plus-guidance strategy.

The symbol explanations in this article are shown in Table 1.

## 2. Problem formulation

We consider a 2-D parabolic PDE system employing moving sensing and actuation components described by

$$v_t(g,k,t) = \sigma\Delta v(g,k,t) + \lambda v(g,k,t) + b^T(g;k;g^a(t);k^a(t))u(t), \tag{2.1}$$

$$y_{ij}(t) = \int_0^\alpha \int_0^\beta c(g;k;g_{ij}^z(t);k_{ij}^z(t))v(g,k,t)\,dg\,dki \in \mathcal{M} \triangleq \{1,2,\ldots,m\}, \quad j \in \mathcal{N} \triangleq \{1,2,\ldots,n\},$$

subject to boundary condition

$$v(g,k,t)|_{\partial W} = 0 \tag{2.2}$$

and initial condition

$$v(g,k,0) = v_0(g,k), \tag{2.3}$$

where $\sigma > 0$ and $\lambda > 0$ are the known constants, $v(g,k,t) \in \mathcal{L}^2(W)$ is the system state, and $(g,k) \in W$ as well as $t \geq 0$ represent the spatial position and time, respectively. The control input $u(t)$ is defined as

$$u(t) \triangleq \left[u_{11}(t)\ u_{12}(t)\cdots u_{1n}(t)\ \ u_{21}(t)\ u_{22}(t)\cdots u_{2n}(t)\ \ \cdots u_{m1}(t)\ u_{m2}(t)\cdots u_{mn}(t)\right]^T \in \mathbb{R}^{mn}.$$

The vector distribution function $b(g;k;g^a(t);k^a(t))$ is presented as

$$\begin{aligned} b(g;k;g^a(t);k^a(t)) \triangleq \Big[&b(g;k;g_{11}^a(t);k_{11}^a(t)),\ldots,b(g;k;g_{1n}^a(t);k_{1n}^a(t)),\\ &b(g;k;g_{21}^a(t);k_{21}^a(t)),\ldots,b(g;k;g_{2n}^a(t);k_{2n}^a(t)),\ldots,\\ &b(g;k;g_{m1}^a(t);k_{m1}^a(t)),\ldots,b(g;k;g_{mn}^a(t);k_{mn}^a(t))\Big]^T \end{aligned}$$

in which $b(g;k;g_{ij}^a(t);k_{ij}^a(t))$ represents the spatial distribution of actuator numbered $ij$, describing the control input $u_{ij}(t)$ is distributed in $W$. $c(g;k;g_{ij}^z(t);k_{ij}^z(t))$ is the spatial distribution of the mobile sensor numbered $ij$. $(g_{ij}^a(t),k_{ij}^a(t))$ and $(g_{ij}^z(t),k_{ij}^z(t))$ specify the differentiable spatial coordinates for the mobile actuator and sensor numbered $ij$ respectively. $y_{ij}(t) \in \mathbb{R}$ is the system measurement output.

In this study, we assume that $g_{ij}^a(t) = g_{ij}^z(t), k_{ij}^a(t) = k_{ij}^z(t), i \in \mathcal{M}, j \in \mathcal{N}$), and $b(g;k;g_{ij}^a(t);k_{ij}^a(t))$ and $c(g;k;g_{ij}^a(t);k_{ij}^a(t))$ are defined as

$$\begin{aligned} b(g;k;g_{ij}^a(t);k_{ij}^a(t)) &= c(g;k;g_{ij}^a(t);k_{ij}^a(t))\\ &\triangleq \begin{cases} 1, & \text{if } |g - g_{ij}^a(t)| < s \text{ and } |k - k_{ij}^a(t)| < s,\\ 0, & \text{otherwise,} \end{cases} \end{aligned} \tag{2.4}$$

where $s > 0$ is a prescribed positive constant characterizing the spatial coverage region of each sensor/actuator pair.

In the following, the well-posedness of the open-loop PDE systems (2.1)–(2.3) within the $C_0$ semigroup framework is discussed. First, we set a trajectory segment $v(t) = v(\cdot,\cdot,t) \triangleq \{v(g,k,t),(g,k) \in W\}$. Under the boundary condition (2.2) and the initial condition (2.3), the abstract evolution equation evolved from PDE (2.1) is given as follows:

$$\begin{aligned} \dot{v}(t) =& \mathcal{A}v(t) + \mathcal{B}(g^a(t),k^a(t))u(t) \\ v(0) =& v_0(\cdot,\cdot), t > 0, \end{aligned} \tag{2.5}$$

where $\mathcal{A}$ is the spatial differential operator defined as

$$\mathcal{A}\bar{v}(g,k) \triangleq \sigma\triangle\bar{v}(g,k) + \lambda\bar{v}(g,k) \tag{2.6}$$

in the domain $\mathcal{D}(\mathcal{A}) \triangleq \{\bar{v} \in \mathcal{H}^2(W) : \frac{\partial\bar{v}(g,k)}{\partial g\partial k}|_{(g,k)\in\partial W} = 0\}$, and the definition of operator $\mathcal{B}(g^a(t);k^a(t))$ is presented in the following:

$$\begin{aligned} \mathcal{B}(g^a(t);k^a(t))u(t) &\triangleq b^T(g;k;g^a(t);k^a(t))u(t) \\ &\triangleq \begin{bmatrix} b(g;k;g^a_{11}(t);k^a_{11}(t)) \\ \vdots \\ b(g;k;g^a_{1n}(t);k^a_{1n}(t)) \\ \vdots \\ b(g;k;g^a_{mn}(t);k^a_{mn}(t)) \end{bmatrix}^T \begin{bmatrix} u_{11}(t) \\ \vdots \\ u_{1n}(t) \\ \vdots \\ u_{mn}(t) \end{bmatrix}. \end{aligned} \tag{2.7}$$

Clearly, the linear operator $\mathcal{B}(g^a(t);k^a(t))$ is bounded. As in [47], the operator $\mathcal{A}$ with $\mathcal{D}(\mathcal{A})$ generates a $C_0$ semigroup $\exp(\mathcal{A}t)$ on $\mathcal{L}^2(W)$. In accordance with Theorem 3.1.3 in [48], it can be easily concluded that Eq (2.5) has a mild solution $v(t)$ on $[0,\infty)$.

Then, we put forward the following static output feedback (SOF) control laws for the systems (2.1)–(2.3):

$$u_{ij}(t) = -l_{ij}y_{ij}(t),\ i \in \mathcal{M}, j \in \mathcal{N} \tag{2.8}$$

where $l_{ij}$, $i \in \mathcal{M}$, $j \in \mathcal{N}$ indicate the control gains to be designed.

In this article, we divide $(0,\alpha)$ into $m$ subintervals with the points $\alpha_1,\alpha_2,\cdots,\alpha_{m+1}$, expressed by $(\alpha_i,\alpha_{i+1})$, $i \in \mathcal{M}$, where $0 = \alpha_1 < \alpha_2 < \cdots < \alpha_{m+1} = \alpha$. Divide $(0,\beta)$ into $n$ subintervals with the points $\beta_1,\beta_2,\cdots,\beta_{n+1}$, denoted by $(\beta_j,\beta_{j+1})$, $j \in \mathcal{N}$, where $0 = \beta_1 < \beta_2 < \cdots < \beta_{n+1} = \beta$. Therefore, the spatial domain $W$ can be divided into $m \times n$ subdomain represented as $W_{ij} \triangleq (\alpha_i,\alpha_{i+1}) \times (\beta_j,\beta_{j+1})$, $i \in \mathcal{M}$, $j \in \mathcal{N}$.

To avoid the collision and achieve the design, the sensor/actuator pair numbered $ij$ is required to move within the spatial domain $W_{ijs} \triangleq (\alpha_i+\iota s,\alpha_{i+1}-\iota s)\times(\beta_j+\iota s,\beta_{j+1}-\iota s) \subset W_{ij}$ (i.e., $(g^a_{ij}(t),k^a_{ij}(t)) \in W_{ijs}$, $i \in \mathcal{M}$, $j \in \mathcal{N}$), where $\iota > 1$ is a design parameter. Further, define the spatial domain $W^a_{ijs}(t) \triangleq (g^a_{ij}(t)-s,g^a_{ij}(t)+s)\times(k^a_{ij}(t)-s,k^a_{ij}(t)+s)$, $i \in \mathcal{M}$, $j \in \mathcal{N}$. To achieve the control design goal, we need to utilize the projection operator idea.

Define the domains $W_{ij\delta} \triangleq (\alpha_i + \iota s + \delta, \alpha_{i+1} - \iota s - \delta) \times (\beta_j + \iota s + \delta, \beta_{j+1} - \iota s - \delta) \subset W_{ijs}$, $i \in \mathcal{M}$, $j \in \mathcal{N}$, where $\delta > 0$ is a design parameter. The following operators are defined for $\varsigma_{ij}, h_{ij} \in \mathbb{R}$, $i \in \mathcal{M}$, $j \in \mathcal{N}$ by using the idea of smoothed projection:

$$\text{Proj}\left(g_{ij}^a(t), \varsigma_{ij}\right) \triangleq \begin{cases} \varsigma_{ij}, & \text{if } \alpha_i + \iota s + \delta \leqslant g_{ij}^a(t) \leqslant \alpha_{i+1} - \iota s - \delta \\ & \text{or if } g_{ij}^a(t) > \alpha_{i+1} - \iota s - \delta \text{ and } \varsigma_{ij} \leqslant 0 \\ & \text{or if } g_{ij}^a(t) < \alpha_i + \iota s + \delta \text{ and } \varsigma_{ij} \geqslant 0 \\ \check{\varsigma}_{ij}, & \text{if } g_{ij}^a(t) < \alpha_i + \iota s + \delta \text{ and } \varsigma_{ij} < 0 \\ \hat{\varsigma}_{ij}, & \text{if } g_{ij}^a(t) > \alpha_{i+1} - \iota s - \delta \text{ and } \varsigma_{ij} > 0, \end{cases} \tag{2.9}$$

where

$$\check{\varsigma}_{ij} = \left[1 + \frac{g_{ij}^a(t) - (\alpha_i + \iota s + \delta)}{\delta}\right] \varsigma_{ij}$$
$$\hat{\varsigma}_{ij} = \left[1 + \frac{(\alpha_{i+1} - \iota s - \delta) - g_{ij}^a(t)}{\delta}\right] \varsigma_{ij},$$

and

$$\text{Proj}\left(k_{ij}^a(t), h_{ij}\right) \triangleq \begin{cases} h_{ij}, & \text{if } \beta_j + \iota s + \delta \leqslant k_{ij}^a(t) \leqslant \beta_{j+1} - \iota s - \delta \\ & \text{or if } k_{ij}^a(t) > \beta_{j+1} - \iota s - \delta \text{ and } h_{ij} \leqslant 0 \\ & \text{or if } k_{ij}^a(t) < \beta_j + \iota s + \delta \text{ and } h_{ij} \geqslant 0 \\ \check{h}_{ij}, & \text{if } k_{ij}^a(t) < \beta_j + \iota s + \delta \text{ and } h_{ij} < 0 \\ \hat{h}_{ij}, & \text{if } k_{ij}^a(t) > \beta_{j+1} - \iota s - \delta \text{ and } h_{ij} > 0, \end{cases} \tag{2.10}$$

where

$$\check{h}_{ij} = \left[1 + \frac{k_{ij}^a(t) - (\beta_j + \iota s + \delta)}{\delta}\right] h_{ij}$$
$$\hat{h}_{ij} = \left[1 + \frac{(\beta_{j+1} - \iota s - \delta) - k_{ij}^a(t)}{\delta}\right] h_{ij}.$$

**Lemma 2.1.** [34] *For each $i \in \mathcal{M}$, $j \in \mathcal{N}$, let $g_{ij}^a(t), k_{ij}^a(t)$ evolve in accordance with the following dynamics:*

$$\dot{g}_{ij}^a(t) = \text{Proj}\left(g_{ij}^a(t), \varsigma_{ij}\right), \ \dot{k}_{ij}^a(t) = \text{Proj}\left(k_{ij}^a(t), h_{ij}\right), \ (g_{ij}^a(0), k_{ij}^a(0)) \in W_{ij\delta}. \tag{2.11}$$

Then, we get the following two results:

(i) $g_{ij}^a(t) \in (\alpha_i + \iota s, \alpha_{i+1} - \iota s)$
$k_{ij}^a(t) \in (\beta_j + \iota s, \beta_{j+1} - \iota s)$
(i.e., $(g_{ij}^a(t), k_{ij}^a(t)) \in W_{ijs}$), $\quad i \in \mathcal{M}, j \in \mathcal{N}$;

(ii) $0 \leqslant \text{Proj}(g_{ij}^a(t), \varsigma_{ij})\varsigma_{ij} \leqslant \varsigma_{ij}^2$
$0 \leqslant \text{Proj}(k_{ij}^a(t), h_{ij})h_{ij} \leqslant h_{ij}^2, \quad i \in \mathcal{M}, j \in \mathcal{N}$.

**Remark 2.1.** The control-plus-guidance design of this study is based on $(g_{ij}^a(t), k_{ij}^a(t)) \in W_{ijs}$, $i \in \mathcal{M}$, $j \in \mathcal{N}$, and the projection approach is used to restrict the moving range of each sensor/actuator pair. In the absence of projection operators defined in (2.9) and (2.10), the designed guidance laws may cause the sensor/actuator pair numbered $ij$ deviates from the predetermined region $W_{ijs}$, which will bring about a collision between actuator/sensor pairs and invalidate the control design method. Moreover, with the increase of the space dimension, the difficulty of both the control and guidance design for PDE systems increases dramatically. Compared with the 1-D space, the 2-D space needs to design the guidance laws from two directions separately. Moreover, the guidance laws of two directions are coupled with each other to jointly realize the guidance problem of the mobile sensor/actuator pairs, which is a typical characteristic for the actual space 2-D PDE systems.

**Lemma 2.2.** *[49] For any $v \in \mathcal{L}^2(W)$, we have*

$$\int_W (v(g,k) - v_W)^2 \, dg \, dk \leq \frac{(\mathrm{dia}(W))^2}{\pi^2} \int_W \nabla v^\top(g,k) \nabla v(g,k) \, dg \, dk, \tag{2.12}$$

*where $v_W \triangleq \frac{1}{\mathrm{leb}(W)} \int_W v(g,k) dg dk$. For any $\overline{W} \subset W$ and any $v \in \mathcal{L}^2(W)$, one has*

$$\int_W (v(g,k) - v_{\overline{W}})^2 \, dg \, dk \leq \frac{4\,\mathrm{leb}(W)(\mathrm{dia}(W))^2}{\mathrm{leb}(\overline{W})\pi^2} \int_W \nabla v^\top(g,k) \nabla v(g,k) \, dg \, dk, \tag{2.13}$$

*where $v_{\overline{W}} \triangleq \frac{1}{\mathrm{leb}(\overline{W})} \int_{\overline{W}} v(g,k) dg dk$.*

Therefore, the goal of this study is to design the SOF controller (2.8) and develop effective guidance laws of mobile sensors/actuators for guaranteeing the asymptotic stability of the spatial 2-D closed-loop PDE systems (2.1)–(2.3).

## 3. Main results

Before the integrated design, it is necessary to analyze the well-posedness of closed-loop space 2-D system. Considering (2.2), (2.4), and (2.6)–(2.8), the closed-loop system (2.1) can be expressed as

$$\dot{v}(t) = \mathcal{A}v(t) + \mathcal{B}(g^a(t), k^a(t))\mathcal{L}\mathcal{C}(g^a(t), k^a(t))v(t), \qquad v(0) = v_0(\cdot,\cdot), \quad t > 0, \tag{3.1}$$

where $\mathcal{L} \triangleq -\mathrm{diag}\,\{l_{11}, l_{12}, \cdots, l_{1n}, l_{21}, l_{22}, \cdots, l_{2n}, \cdots, l_{m1}, l_{m2}, \cdots, l_{mn}\}$, and the definition of $C(g^a(t); k^a(t))$ is presented as follows:

$$C(g^a(t),k^a(t))v(t) \triangleq \begin{bmatrix} \int_{g^a_{11}(t)-s}^{g^a_{11}(t)+s} \int_{k^a_{11}(t)-s}^{k^a_{11}(t)+s} v(g,k,t)\,dg\,dk \\ \vdots \\ \int_{g^a_{1n}(t)-s}^{g^a_{1n}(t)+s} \int_{k^a_{1n}(t)-s}^{k^a_{1n}(t)+s} v(g,k,t)\,dg\,dk \\ \vdots \\ \int_{g^a_{m1}(t)-s}^{g^a_{m1}(t)+s} \int_{k^a_{m1}(t)-s}^{k^a_{m1}(t)+s} v(g,k,t)\,dg\,dk \\ \vdots \\ \int_{g^a_{mn}(t)-s}^{g^a_{mn}(t)+s} \int_{k^a_{mn}(t)-s}^{k^a_{mn}(t)+s} v(g,k,t)\,dg\,dk \end{bmatrix}. \tag{3.2}$$

According to (2.4), it can be concluded that $\mathcal{B}(g^a(t),k^a(t))\mathcal{LC}(g^a(t),k^a(t))$ is bounded and continuous in $t$ on $[0,\infty)$. Therefore, in the light of Theorem 1.2 of [50], we can directly draw the conclusion that for each initial value $v_0(\cdot)\in\mathcal{L}^2(W)$, there exists a unique mild solution $v(t)$ for (3.1).

Then, to the control goal, we construct the candidate functional as

$$V(t)=V_1(t)+V_2(t)+V_3(t), \tag{3.3}$$

where

$$V_1(t)=\frac{\tau_1}{2}\int_W v^2(g,k,t)dgdk, \tag{3.4}$$

$$V_2(t)=-\frac{\tau_2}{2}\sum_{i=1}^{m}\sum_{j=1}^{n}\Big(\int_{W^a_{ijs}(t)} v(g,k,t)dgdk\Big)^2, \tag{3.5}$$

$$V_3(t)=\frac{\tau_3}{2}\int_W \nabla v^T(g,k,t)\nabla v(g,k,t)dgdk, \tag{3.6}$$

in which $\tau_1>0$, $0<\tau_2<\frac{\tau_1}{4s^2}$ and $\tau_3>0$ are the constants to be determined.

Provided $(g^a_{ij}(t),k^a_{ij}(t))\in W_{ijs}$, it is easy to get $(g^a_{ij}(t)-s,g^a_{ij}(t)+s)\times(k^a_{ij}(t)-s,k^a_{ij}(t)+s)\subset(\alpha_i,\alpha_{i+1})\times(\beta_j,\beta_{j+1})$, $i\in\mathcal{M}$, $j\in\mathcal{N}$. Based on the Cauchy–Schwarz inequality, we have

$$\begin{aligned} &-\left(\int_{W^a_{ijs}(t)} v(g,k,t)\,dg\,dk\right)^2 \\ \geq&-4s^2\int_{W^a_{ijs}(t)} v^2(g,k,t)\,dg\,dk \\ \geq&-4s^2\int_{W_{ij}} v^2(g,k,t)\,dg\,dk. \end{aligned} \tag{3.7}$$

Thus, from (3.3) and (3.7), we get

$$V(t) \geq \frac{(\tau_1 - 4s^2\tau_2)}{2} \int_W v^2(g,k,t)\,dg\,dk + \frac{\tau_3}{2} \int_W \nabla v^\top(g,k,t)\nabla v(g,k,t)\,dg\,dk, \tag{3.8}$$

where $\tau_1 - 4s^2\tau_2 > 0$.

Then, by taking the time derivative of $V_1(t)$ along the solution to (2.1)–(2.3) under (2.4) and (2.8), we acquire

$$\begin{aligned}
\dot{V}_1(t) &= \tau_1 \int_W v(g,k,t)v_t(g,k,t)\,dg\,dk \\
&= \tau_1 \int_W v(g,k,t)\Big[\sigma\Delta v(g,k,t) + \lambda v(g,k,t) \\
&\quad - \sum_{i=1}^{m}\sum_{j=1}^{n} b(g;k;g_{ij}^a(t);k_{ij}^a(t))l_{ij} \int_{W_{ijs}^a(t)} v(g,k,t)\,dg\,dk\Big]\,dg\,dk \\
&= \tau_1\sigma \int_W v(g,k,t)\Delta v(g,k,t)\,dg\,dk + \tau_1\lambda \int_W v^2(g,k,t)\,dg\,dk \\
&\quad - \tau_1 \sum_{i=1}^{m}\sum_{j=1}^{n} l_{ij}\Big(\int_{W_{ijs}^a(t)} v(g,k,t)\,dg\,dk\Big)^2.
\end{aligned} \tag{3.9}$$

Based on the boundary condition (2.2) and applying Green's formula, one has

$$\int_W v(g,k,t)\Delta v(g,k,t)\,dg\,dk = -\int_W \nabla v^\top(g,k,t)\nabla v(g,k,t)\,dg\,dk. \tag{3.10}$$

Substituting (3.10) into (3.9), one can get

$$\begin{aligned}
\dot{V}_1(t) &= -\sigma\tau_1 \sum_{i=1}^{m}\sum_{j=1}^{n} \int_{W_{ij}} \nabla v^\top(g,k,t)\nabla v(g,k,t)\,dg\,dk \\
&\quad + \lambda\tau_1 \sum_{i=1}^{m}\sum_{j=1}^{n} \int_{W_{ij}} v^2(g,k,t)\,dg\,dk \\
&\quad - \tau_1 \sum_{i=1}^{m}\sum_{j=1}^{n} l_{ij}\Big(\int_{W_{ijs}^a(t)} v(g,k,t)\,dg\,dk\Big)^2.
\end{aligned} \tag{3.11}$$

By the inequality (2.13) in Lemma 2.2 and considering $W_{ijs}^a(t) \subset W_{ij}$, $i \in \mathcal{M}$, $j \in \mathcal{N}$, for any $W_{ij}$, we obtain

$$\int_{W_{ij}} \nabla v^\top(g,k,t)\nabla v(g,k,t)\,dgdk \geq \frac{\pi^2}{\xi_{ij}} \int_{W_{ij}} \Big[v(g,k,t) - \frac{\int_{W_{ijs}^a(t)} v(g,k,t)\,dgdk}{\mathrm{leb}(W_{ijs}^a(t))}\Big]^2 dgdk, \tag{3.12}$$

where $\xi_{ij} \triangleq \frac{4\mathrm{leb}(W_{ij})(\mathrm{dia}W_{ij})^2}{\mathrm{leb}(W_{ijs}^a(t))}$, $\frac{1}{\mathrm{leb}(W_{ijs}^a(t))} = \frac{1}{4s^2}$. With (3.12), $\dot{V}_1(t)$ is written as

$$\begin{aligned}\dot{V}_1(t) \leq & -\sigma\tau_1 \sum_{i=1}^{m}\sum_{j=1}^{n}\frac{\pi^2}{\xi_{ij}}\int_{W_{ij}}\Big[v(g,k,t)-\frac{1}{4s^2}\int_{W^a_{ijs}(t)}v(g,k,t)\,dgdk\Big]^2 dgdk \\ & +\lambda\tau_1\sum_{i=1}^{m}\sum_{j=1}^{n}\int_{W_{ij}}v^2(g,k,t)\,dgdk \\ & -\tau_1\sum_{i=1}^{m}\sum_{j=1}^{n}l_{ij}\Big(\int_{W^a_{ijs}(t)}v(g,k,t)\,dgdk\Big)^2.\end{aligned} \tag{3.13}$$

Set

$$\Phi^{ij}(g,t)=\int_{k^a_{ij}(t)-s}^{k^a_{ij}(t)+s}v(g,k,t)dk,\ i\in\mathcal{M},\ j\in\mathcal{N} \tag{3.14}$$

and the derivatives of $\Phi^{ij}(g,t),\ i\in\mathcal{M},\ j\in\mathcal{N}$ are

$$\begin{aligned}\Phi^{ij}_t(g,t)=&\int_{k^a_{ij}(t)-s}^{k^a_{ij}(t)+s}v_t(g,k,t)dk+v(g,k^a_{ij}(t)+s,t)\dot{k}^a_{ij}(t)\\ &-v(g,k^a_{ij}(t)-s,t)\dot{k}^a_{ij}(t),\ i\in\mathcal{M},\ j\in\mathcal{N}.\end{aligned} \tag{3.15}$$

Thus, substitute (3.14) into (3.5) to get

$$V_2(t)=-\frac{\tau_2}{2}\sum_{i=1}^{m}\sum_{j=1}^{n}\Big(\int_{g^a_{ij}(t)-s}^{g^a_{ij}(t)+s}\Phi^{ij}(g,t)dg\Big)^2. \tag{3.16}$$

With (3.14)–(3.16), we can get

$$\begin{aligned}\dot{V}_2(t)=&-\tau_2\sum_{i=1}^{m}\sum_{j=1}^{n}\int_{g^a_{ij}(t)-s}^{g^a_{ij}(t)+s}\Phi^{ij}(g,t)\,dg\\ &\times\Big\{\int_{g^a_{ij}(t)-s}^{g^a_{ij}(t)+s}\Phi^{ij}_t(g,t)\,dg+\Phi^{ij}(g^a_{ij}(t)+s,t)\dot{g}^a_{ij}(t)-\Phi^{ij}(g^a_{ij}(t)-s,t)\dot{g}^a_{ij}(t)\Big\}\\ =&-\tau_2\sum_{i=1}^{m}\sum_{j=1}^{n}\int_{W^a_{ijs}(t)}v(g,k,t)\,dg\,dk\times\Big\{\int_{W^a_{ijs}(t)}v_t(g,k,t)\,dg\,dk\\ &+\dot{k}^a_{ij}(t)\int_{g^a_{ij}(t)-s}^{g^a_{ij}(t)+s}\Big[v(g,k^a_{ij}(t)+s,t)-v(g,k^a_{ij}(t)-s,t)\Big]dg\\ &+\dot{g}^a_{ij}(t)\int_{k^a_{ij}(t)-s}^{k^a_{ij}(t)+s}\Big[v(g^a_{ij}(t)+s,k,t)-v(g^a_{ij}(t)-s,k,t)\Big]dk\Big\}.\end{aligned} \tag{3.17}$$

Similar to (3.10), $\dot{V}_3(t)$ can be obtained as

$$\begin{aligned}\dot{V}_3(t)=&\tau_3\int_W\nabla v^T(g,k,t)\nabla v_t(g,k,t)dgdk\\ =&-\tau_3\int_W\Delta v(g,k,t)v_t(g,k,t)dgdk.\end{aligned} \tag{3.18}$$

Thus, integrating (2.1), (2.4), and (2.8) into (3.18) yields that

$$\begin{aligned}\dot{V}_3(t) =&\frac{\tau_3}{\sigma}\int_W\Big[-v_t^2(g,k,t)+\lambda v(g,k,t)v_t(g,k,t)\\&-v_t(g,k,t)\sum_{i=1}^{m}\sum_{j=1}^{n}l_{ij}b(g;k;g_{ij}^a(t);k_{ij}^a(t))\int_{W_{ijs}^a(t)}v(g,k,t)\,dg\,dk\Big]\,dg\,dk\\=&-\frac{\tau_3\eta}{\sigma}\sum_{i=1}^{m}\sum_{j=1}^{n}\int_{W_{ij}}v_t^2(g,k,t)\,dg\,dk\\&-\frac{\tau_3(1-\eta)}{\sigma}\sum_{i=1}^{m}\sum_{j=1}^{n}\int_{W_{ij}}v_t^2(g,k,t)\,dg\,dk\\&+\frac{\tau_3}{\sigma}\sum_{i=1}^{m}\sum_{j=1}^{n}\int_{W_{ij}}\lambda v(g,k,t)v_t(g,k,t)\,dg\,dk\\&-\frac{\tau_3}{\sigma}\sum_{i=1}^{m}\sum_{j=1}^{n}\int_{W_{ij}}\Big[v_t(g,k,t)\sum_{p=1}^{m}\sum_{q=1}^{n}l_{pq}b(g;k;g_{pq}^a(t);k_{pq}^a(t))\\&\times\int_{W_{pqs}^a(t)}v(g,k,t)\,dg\,dk\Big]\,dg\,dk,\end{aligned}\tag{3.19}$$

where $0<\eta<1$.

Following the same approach as in (3.7), we derive

$$\begin{aligned}&-\Big(\int_{W_{ijs}^a(t)}v_t(g,k,t)\,dg\,dk\Big)^2\\&\geq -4s^2\int_{W_{ijs}^a(t)}v_t^2(g,k,t)\,dg\,dk\\&\geq -4s^2\int_{W_{ij}}v_t^2(g,k,t)\,dg\,dk.\end{aligned}\tag{3.20}$$

By applying inequality (3.20), $\dot{V}_3(t)$ is rewritten as

$$\begin{aligned}\dot{V}_3(t)\leq&-\frac{\tau_3\eta}{\sigma}\sum_{i=1}^{m}\sum_{j=1}^{n}\int_{W_{ij}}v_t^2(g,k,t)\,dg\,dk\\&-\frac{\tau_3(1-\eta)}{4\sigma s^2}\sum_{i=1}^{m}\sum_{j=1}^{n}\Big(\int_{W_{ijs}^a(t)}v_t(g,k,t)\,dg\,dk\Big)^2\\&+\frac{\tau_3}{\sigma}\sum_{i=1}^{m}\sum_{j=1}^{n}\int_{W_{ij}}\lambda v(g,k,t)v_t(g,k,t)\,dg\,dk\\&-\frac{\tau_3}{\sigma}\sum_{i=1}^{m}\sum_{j=1}^{n}l_{ij}\int_{W_{ijs}^a(t)}v_t(g,k,t)\,dg\,dk\int_{W_{ijs}^a(t)}v(g,k,t)\,dg\,dk.\end{aligned}\tag{3.21}$$

From (3.13), (3.17), and (3.21), we get

$$\begin{aligned}\dot{V}(t) \leq & \sum_{i=1}^{m}\sum_{j=1}^{n}\int_{W_{ij}}\tilde{v}^{\top}(g,k,t)\Upsilon_{ij}\tilde{v}(g,k,t)\,dg\,dk \\ & + \tau_2\sum_{i=1}^{m}\sum_{j=1}^{n}\int_{W^a_{ijs}(t)}v(g,k,t)\,dg\,dk \\ & \times\Big\{\dot{k}^a_{ij}(t)\int_{g^a_{ij}(t)-s}^{g^a_{ij}(t)+s}\Big[v(g,k^a_{ij}(t)-s,t)-v(g,k^a_{ij}(t)+s,t)\Big]dg \\ & + \dot{g}^a_{ij}(t)\int_{k^a_{ij}(t)-s}^{k^a_{ij}(t)+s}\Big[v(g^a_{ij}(t)-s,k,t)-v(g^a_{ij}(t)+s,k,t)\Big]dk\Big\},\end{aligned} \tag{3.22}$$

where

$$\tilde{v}(g,k,t)\triangleq\Big[v(g,k,t),\quad v_t(g,k,t),\quad \int_{W^a_{ijs}(t)}v(g,k,t)\,dg\,dk,\quad \int_{W^a_{ijs}(t)}v_t(g,k,t)\,dg\,dk\Big]^{\top}$$

and

$$\Upsilon_{ij}\triangleq\begin{bmatrix}\Upsilon_{ij,11} & \Upsilon_{ij,12} & \Upsilon_{ij,13} & 0\\ * & \Upsilon_{ij,22} & 0 & 0\\ * & * & \Upsilon_{ij,33} & \Upsilon_{ij,34}\\ * & * & * & \Upsilon_{ij,44}\end{bmatrix} \tag{3.23}$$

with

$$\begin{aligned}&\Upsilon_{ij,11}\triangleq-\frac{\tau_1\pi^2\sigma}{\xi_{ij}}+\lambda\tau_1,\ \Upsilon_{ij,12}\triangleq\frac{\lambda\tau_3}{2\sigma}\\ &\Upsilon_{ij,13}\triangleq\frac{\tau_1\pi^2\sigma}{4s^2\xi_{ij}},\ \Upsilon_{ij,22}\triangleq-\frac{\eta\tau_3}{\sigma}\\ &\Upsilon_{ij,33}\triangleq-\frac{\tau_1\pi^2\sigma}{16s^4\xi_{ij}}-\frac{l_{ij}\tau_1}{\mathrm{leb}(W_{ij})}\\ &\Upsilon_{ij,34}\triangleq-\frac{\tau_2}{2\mathrm{leb}(W_{ij})}-\frac{\tau_3 l_{ij}}{2s\sigma\mathrm{leb}(W_{ij})}\\ &\Upsilon_{ij,44}\triangleq-\frac{(1-\eta)\tau_3}{4s^2\sigma\mathrm{leb}(W_{ij})}.\end{aligned} \tag{3.24}$$

In addition, to guarantee $(g^a_{ij}(t),k^a_{ij}(t))\in W_{ijs}$, the following sensor/actuator guidance laws are presented:

$$\begin{aligned}&\dot{g}^a_{ij}(t)=\mathrm{Proj}\,(g^a_{ij}(t),\varsigma_{ij}),\qquad \dot{k}^a_{ij}(t)=\mathrm{Proj}\,(k^a_{ij}(t),h_{ij})\\ &(g^a_{ij}(0),k^a_{ij}(0))\in W_{ij\delta},\quad i\in\mathcal{M},\ j\in\mathcal{N},\end{aligned} \tag{3.25}$$

where

$$\begin{aligned}\varsigma_{ij} &= -\mu_{ij}\Big[\int_{k_{ij}^a(t)-s}^{k_{ij}^a(t)+s}\Big(v(g_{ij}^a(t)-s,k,t)-v(g_{ij}^a(t)+s,k,t)\Big)dk\Big]y_{ij}(t),\quad i\in\mathcal{M}, j\in\mathcal{N}\\ h_{ij} &= -\varphi_{ij}\Big[\int_{g_{ij}^a(t)-s}^{g_{ij}^a(t)+s}\Big(v(g,k_{ij}^a(t)-s,t)-v(g,k_{ij}^a(t)+s,t)\Big)dg\Big]y_{ij}(t),\quad i\in\mathcal{M}, j\in\mathcal{N}\end{aligned}\tag{3.26}$$

in which $\mu_{ij}>0,\varphi_{ij}>0, i\in\mathcal{M}, j\in\mathcal{N}$ indicate adjustable parameters.

**Theorem 3.1.** *Given the scalars $0<\eta<1$, $s>0$, $\sigma>0$, $\lambda>0$, $\alpha_1,\alpha_2,\ldots,\alpha_{m+1}$, and $\beta_1,\beta_2,\ldots,\beta_{n+1}$, assume that there are scalars $\bar{\tau}_1>0,\bar{\tau}_2>0,\bar{\tau}_3>0$ and $\bar{l}_{ij}$, which can ensure that the following inequalities hold:*

$$\bar{\tau}_3-4s^2\bar{\tau}_2>0,\tag{3.27}$$

*and*

$$\bar{\Upsilon}_{ij}\triangleq\begin{bmatrix}\bar{\Upsilon}_{ij,11} & \bar{\Upsilon}_{ij,12} & \bar{\Upsilon}_{ij,13} & 0\\ * & \bar{\Upsilon}_{ij,22} & 0 & 0\\ * & * & \bar{\Upsilon}_{ij,33} & \bar{\Upsilon}_{ij,34}\\ * & * & * & \bar{\Upsilon}_{ij,44}\end{bmatrix}<0\tag{3.28}$$

*with*

$$\begin{aligned}\bar{\Upsilon}_{ij,11} &\triangleq -\frac{\bar{\tau}_1\pi^2\sigma}{\xi_{ij}}+\lambda\bar{\tau}_1,\ \bar{\Upsilon}_{ij,12}\triangleq\frac{\lambda\bar{\tau}_1}{2\sigma}\\ \bar{\Upsilon}_{ij,13} &\triangleq \frac{\bar{\tau}_1\pi^2\sigma}{4s^2\xi_{ij}},\ \bar{\Upsilon}_{ij,22}\triangleq-\frac{\eta\bar{\tau}_3}{\sigma}\\ \bar{\Upsilon}_{ij,33} &\triangleq -\frac{\bar{\tau}_1\pi^2\sigma}{16s^4\xi_{ij}}-\frac{\bar{l}_{ij}}{\mathrm{leb}(W_{ij})}\\ \bar{\Upsilon}_{ij,34} &\triangleq -\frac{\bar{\tau}_2}{2\mathrm{leb}(W_{ij})}-\frac{\bar{l}_{ij}}{2\sigma\mathrm{leb}(W_{ij})}\\ \bar{\Upsilon}_{ij,44} &\triangleq -\frac{(1-\eta)\bar{\tau}_3}{4s^2\sigma\mathrm{leb}(W_{ij})}.\end{aligned}\tag{3.29}$$

*Then, the closed-loop system can achieve the asymptotic stability through the synthesized SOF controllers (2.8) with the gains*

$$l_{ij}=\bar{\tau}_1^{-1}\bar{l}_{ij}\tag{3.30}$$

*and the coordinated sensor/actuator guidance laws (3.25) with (3.26).*

*Proof.* Set

$$\begin{aligned}\bar{\tau}_1=\tau_1^{-1},\qquad \bar{\tau}_2=\tau_1^{-1}\tau_2\tau_3^{-1}\\ \bar{\tau}_3=\tau_3^{-1},\qquad \bar{l}_{ij}=l_{ij}\bar{\tau}_1,\quad i\in\mathcal{M},\ j\in\mathcal{N}.\end{aligned}\tag{3.31}$$

Together with (3.31), we can get about the matrices $\Upsilon_{ij}$ in (3.23) that

$$\bar{\Upsilon}_{ij} \triangleq R\Upsilon_{ij}R, \tag{3.32}$$

where $R \triangleq \text{diag}\{\bar{\tau}_1, \bar{\tau}_3, \bar{\tau}_1, \bar{\tau}_3\} > 0$. Moreover, according to (3.25) and conclusion (ii) in Lemma 2.1, we get

$$\begin{aligned}
&\tau_2 \sum_{i=1}^{m}\sum_{j=1}^{n} \dot{g}_{ij}^a(t) \int_{W_{ijs}(t)} v(g,k,t)\,dg\,dk \\
&\quad \times \int_{k_{ij}^a(t)-s}^{k_{ij}^a(t)+s} \Big[v(g_{ij}^a(t)-s,k,t) - v(g_{ij}^a(t)+s,k,t)\Big]\,dk \\
&= -\sum_{i=1}^{m}\sum_{j=1}^{n} \frac{\tau_2}{\mu_{ij}} \text{Proj}\,(g_{ij}^a(t), \varsigma_{ij})\varsigma_{ij} \\
&\le 0
\end{aligned} \tag{3.33}$$

and

$$\begin{aligned}
&\tau_2 \sum_{i=1}^{m}\sum_{j=1}^{n} \dot{k}_{ij}^a(t) \int_{W_{ijs}(t)} v(g,k,t)\,dg\,dk \\
&\quad \times \int_{g_{ij}^a(t)-s}^{g_{ij}^a(t)+s} \Big[v(g,k_{ij}^a(t)-s,t) - v(g,k_{ij}^a(t)+s,t)\Big]\,dg \\
&= -\sum_{i=1}^{m}\sum_{j=1}^{n} \frac{\tau_2}{\varphi_{ij}} \text{Proj}\,(k_{ij}^a(t), h_{ij})h_{ij} \\
&\le 0.
\end{aligned} \tag{3.34}$$

Based on (3.28) and (3.32), the following inequalities can be easily obtained:

$$\Upsilon_{ij} + \omega I \le 0, \qquad i \in \mathcal{M},\ j \in \mathcal{N}, \tag{3.35}$$

where $\omega$ is a sufficiently small scalar. Thus, it follows from (3.22), (3.33)–(3.35) that

$$\begin{aligned}
\dot{V}(t) &\le -\omega \sum_{i=1}^{m}\sum_{j=1}^{n} \int_{W_{ij}} \tilde{v}^\top(g,k,t)\tilde{v}(g,k,t)\,dg\,dk \\
&\le -\omega \sum_{i=1}^{m}\sum_{j=1}^{n} \int_{W_{ij}} v^2(g,k,t)\,dg\,dk.
\end{aligned} \tag{3.36}$$

Therefore, from (3.4) and (3.36),

$$\dot{V}(t) \le -\vartheta\frac{\tau_1}{2}\int_W v^2(g,k,t)\,dg\,dk \le -\vartheta V_1(t), \tag{3.37}$$

where $\vartheta = \frac{2\omega}{\tau_1}$, which means

$$\dot{V}(t) \le -\vartheta|v(\cdot,\cdot,t)|_2^2 \le 0. \tag{3.38}$$

From (3.4), (3.37), and (3.38), we can easily get that $V(t)$ is positive definite, and that $\dot{V}(t)$ is negative semi-definite and uniformly continuous with respect to time $t$. According to Barbalat's lemma, it is obvious that $\lim_{t\to\infty} \dot{V}(t) = 0$, and the closed-loop system is asymptotically stable. Furthermore, the control gains in (3.30) can be easily obtained by (3.31). □

In addition, the following assumption is put forward to realize the guidance. The actuator/sensor pair numbered $ij$ is able to obtain state information as follows:

$$\begin{aligned} v_{rh}(t) &= v(g_{ij}^a(t) + s, k_{ij}^a(t) + s, t) \\ v_{rb}(t) &= v(g_{ij}^a(t) + s, k_{ij}^a(t) - s, t) \\ v_{lh}(t) &= v(g_{ij}^a(t) - s, k_{ij}^a(t) + s, t) \\ v_{lb}(t) &= v(g_{ij}^a(t) - s, k_{ij}^a(t) - s, t). \end{aligned} \tag{3.39}$$

Then, the averaged measurements $y_{ij}(t), i \in \mathcal{M}, j \in \mathcal{N}$ can be expressed as

$$\begin{aligned} y_{ij}(t) &= \int_{g_{ij}^a(t)-s}^{g_{ij}^a(t)+s} \int_{k_{ij}^a(t)-s}^{k_{ij}^a(t)+s} v(g,k,t)\, dg\, dk \\ &\simeq 2s \times 2s \frac{v_{rh}(t) + v_{rb}(t) + v_{lh}(t) + v_{lb}(t)}{4} \\ &= s^2\Big[v_{rh}(t) + v_{rb}(t) + v_{lh}(t) + v_{lb}(t)\Big], \quad i \in \mathcal{M},\ j \in \mathcal{N}. \end{aligned} \tag{3.40}$$

Therefore, the availability of $v(g_{ij}^a(t) + s, k_{ij}^a(t) + s, t)$, $v(g_{ij}^a(t) + s, k_{ij}^a(t) - s, t)$,$v(g_{ij}^a(t) - s, k_{ij}^a(t) + s, t)$ and $v(g_{ij}^a(t)-s, k_{ij}^a(t)-s, t)$ would yield the averaged measurements $y_{ij}(t), i \in \mathcal{M}, j \in \mathcal{N}$. In fact, this research presents a novel solution to the spatial sensing requirements defined in (3.26) for implementing the guidance laws (3.25) through an advanced tetra-probe measurement mode. The proposed design utilizes four point sensors arranged in an optimized planar array geometry for enabling accurate field reconstruction at the measurement point through the corresponding data collection algorithm.

**Remark 3.1.** In practice, incorporating velocity saturation dynamics in mobile sensor/actuator pairs is crucial for practical implementation. Similar to the discussion in [33] for the 1-D system, when the mobile sensor/actuator pairs have velocity constraints, the guidance laws (3.25) can be rewritten as follows:

$$\begin{aligned} \dot{g}_{ij}^a(t) = \mathrm{Proj}\left(g_{ij}^a(t), \mathrm{sat}(\varsigma_{ij})\right), \qquad \dot{k}_{ij}^a(t) = \mathrm{Proj}\left(k_{ij}^a(t), \mathrm{sat}(h_{ij})\right) \\ (g_{ij}^a(0), k_{ij}^a(0)) \in W_{ij\delta}, \quad i \in \mathcal{M},\ j \in \mathcal{N}, \end{aligned} \tag{3.41}$$

where

$$\begin{aligned} \mathrm{sat}(\varsigma_{ij}) &= \begin{cases} \varsigma_{ij}, & \text{if } |\varsigma_{ij}| \le \varsigma_{max} \\ \varsigma_{max}\dfrac{\varsigma_{ij}}{|\varsigma_{ij}|}, & \text{if } |\varsigma_{ij}| > \varsigma_{max} \end{cases} \\ \mathrm{sat}(h_{ij}) &= \begin{cases} h_{ij}, & \text{if } |h_{ij}| \le h_{max} \\ h_{max}\dfrac{h_{ij}}{|h_{ij}|}, & \text{if } |h_{ij}| > h_{max} \end{cases} \end{aligned} \tag{3.42}$$

in which $\varsigma_{max} > 0$ and $h_{max} > 0$ are the given positive scalars and respectively represent the maximum allowable velocities in $p$ and $k$ directions. The proposed guidance laws above explicitly account for these physical limitations, which frequently occur in real-world applications due to power restrictions, mechanical design constraints, or operational safety requirements.

**Remark 3.2.** This work addresses the stabilization problem for 2-D linear open-loop unstable PDE systems by developing an integrated control and guidance framework. The proposed methodology achieves asymptotic stability of the closed-loop system while offering significantly broader applicability than conventional approaches. This research not only resolves the distributed control synthesis challenge for 2-D linear PDE systems, but it also implements coordinated spatial navigation for mobile collocated sensor/actuator pairs. A rigorous well-posedness analysis is provided for both open-loop and closed-loop configurations involving moving sensing/actuation elements. Furthermore, the established theoretical framework creates a foundational platform for future extensions to other types of PDE systems, nonlinear stochastic PDE systems by referring to the methods in [51–53], and reinforcement learning-based mobile control [54].

**Remark 3.3.** This study introduces a simplified modeling framework for mobile sensor/actuator pairs in spatially DPSs, treating each pair as massless and inertia-free to allow instantaneous repositioning. Unlike conventional finite-dimensional systems that explicitly model interagent collision avoidance and complex communication protocols, our framework strategically simplifies the problem formulation by neglecting kinematic constraints. This methodological simplification enables the derivation of analytically tractable solutions for the integrated design problem while maintaining mathematical rigor. The proposed mobile sensor/actuator pairs are designed to operate within their respective 2-D subdomains, where they perform dual functions of distributed state estimation and spatially targeted control actuation. Key application scenarios include environmental monitoring and control tasks such as contaminant plume confinement, toxic substance neutralization, dynamic target tracking, and spatially distributed process regulation. Although the present theoretical framework employs these simplifying assumptions to establish fundamental control principles, the ongoing research direction focuses on incorporating realistic kinematic models that account for the physical constraints of mobile platforms. This evolutionary development will significantly enhance the practical applicability of the current framework by addressing real-world implementation challenges such as finite maneuverability, energy-aware deployment strategies, and adaptive interaction with dynamic environments. Moreover, future work will particularly emphasize the development of hierarchical control architectures that combine the current theoretical insights with advanced motion planning algorithms, actuator dynamics compensation, and environment-aware operational protocols, thereby creating a comprehensive solution for complex field deployment scenarios across various engineering domains.

**Remark 3.4.** This work is concerned with modeling DPSs through spatial 2-D PDEs, which provide fundamentally greater physical fidelity than space 1-D models. Compared with 1-D formulations that impose artificial constraints by restricting dynamics to a single spatial axis, our 2-D framework naturally represents the planar interactions characteristic of real-world phenomena, particularly modeling the chemical reaction–diffusion process and gas diffusion process. The developed control methodology introduces innovative bidirectional guidance algorithms that are physically realized through the coordinated mobility of sensor/actuator pairs, enabling these agents to dynamically reconfigure their spatial distribution in response to evolving field conditions. This represents a

paradigm shift from conventional static deployment strategies, as the proposed mobile sensor/actuator pairs offer not only enhanced spatial coverage but also critical capability to actively pursue regions of interest within the space domain. Such dynamic reconfigurability leads to substantial improvements in both state estimation accuracy and control performance for engineering applications, including thermal management systems, pollutant dispersion monitoring, and distributed chemical synthesis processes.

## 4. Numerical simulations

Consider the PDE systems (2.1)–(2.3) under $\sigma = 0.025, \lambda = 0.004$ in the spatial domain $W = (0,1) \times (0,1)$. We select four mobile sensor/actuator pairs with $m = 2$ and $n = 2$, and set the initial condition as $v_0(g,k) = 2.5 - 2.5\cos(2\pi g)\cos(2\pi k)$. Based on the above situations, it can be seen from Figure 1 that the open-loop systems (2.1)–(2.3) are unstable.

Set

$$\begin{gathered} s = 0.06, \quad \iota = 1.10, \quad \delta = 0.02 \\ \varphi_{11} = 50, \quad \varphi_{12} = 70, \quad \varphi_{21} = 50, \quad \varphi_{22} = 50 \\ \mu_{11} = 60, \quad \mu_{12} = 70, \quad \mu_{21} = 90, \quad \mu_{22} = 70 \\ W_{11} = (0, 0.4) \times (0, 0.6), \qquad W_{12} = (0, 0.4) \times (0.6, 1) \\ W_{21} = (0.4, 1) \times (0, 0.6), \qquad W_{22} = (0.4, 1) \times (0.6, 1). \end{gathered}$$

Then, we can get

$$\begin{gathered} W_{11s} = (0.066, 0.334) \times (0.066, 0.534) \\ W_{12s} = (0.066, 0.334) \times (0.666, 0.934) \\ W_{21s} = (0.466, 0.934) \times (0.066, 0.534) \\ W_{22s} = (0.466, 0.934) \times (0.666, 0.934) \end{gathered}$$

and

$$\begin{gathered} W_{11\delta} = (0.086, 0.314) \times (0.086, 0.514) \\ W_{12\delta} = (0.086, 0.314) \times (0.686, 0.914) \\ W_{21\delta} = (0.486, 0.914) \times (0.086, 0.514) \\ W_{22\delta} = (0.486, 0.914) \times (0.686, 0.914). \end{gathered}$$

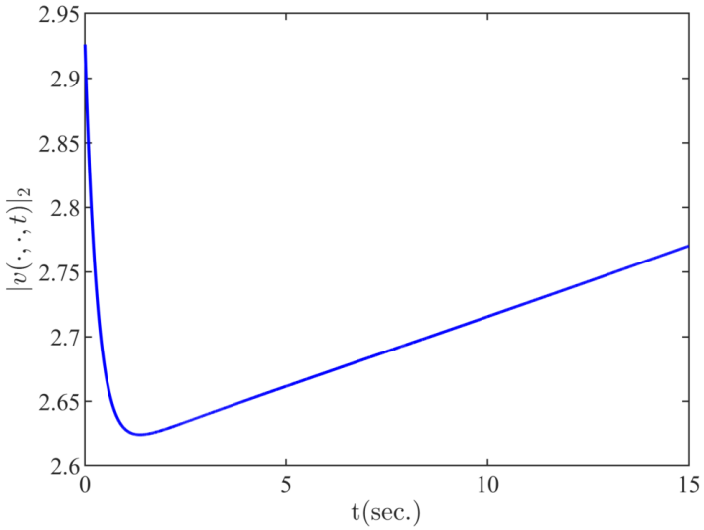


**Figure 1.** Open-loop state norm $|v(\cdot,\cdot,t)|_2$.

The following initial positions for moving actuator/sensor pairs are selected:

$$\begin{aligned}&(g^a_{11}(0), k^a_{11}(0)) = (0.203, 0.416) \in W_{11\delta}, \quad (g^a_{12}(0), k^a_{12}(0)) = (0.169, 0.762) \in W_{12\delta}\\ &(g^a_{21}(0), k^a_{21}(0)) = (0.774, 0.398) \in W_{21\delta}, \quad (g^a_{22}(0), k^a_{22}(0)) = (0.821, 0.755) \in W_{22\delta}.\end{aligned} \tag{4.1}$$

By simple calculation, we have

$$\begin{aligned}&\text{leb}(W_{11}) = 0.24, \quad \text{leb}(W_{12}) = 0.16\\ &\text{leb}(W_{21}) = 0.36, \quad \text{leb}(W_{22}) = 0.24\\ &\text{dia}(W_{11}) = \sqrt{0.52}, \quad \text{dia}(W_{12}) = \sqrt{0.32}\\ &\text{dia}(W_{21}) = \sqrt{0.72}, \quad \text{dia}(W_{22}) = \sqrt{0.52}\\ &\text{leb}(W_{ijs}(t)) = 0.0144, \quad \text{for } i, j \in \{1, 2\}.\end{aligned}$$

By solving LMIs (3.27) and (3.28), we obtain

$$\begin{aligned}&l_{11} = 422.1001, \ l_{12} = 305.5037\\ &l_{21} = 591.5282, \ l_{22} = 417.8664.\end{aligned} \tag{4.2}$$

The simulation results confirm the effectiveness of the proposed integrated control and guidance approach. Specifically, Figure 2 illustrates the asymptotic convergence of the spatial $\mathcal{L}^2$-norm $|v(\cdot,\cdot,t)|_2$, explicitly demonstrating the stabilization capability of the synthesized SOF controllers contrasted with the divergent open-loop dynamics in Figure 1. Figure 3 displays the associated control inputs $u_{ij}(t)$, which dynamically adjust to localized measurements and smoothly converge to zero without severe high-frequency chattering, thereby satisfying practical energy constraints. Furthermore, Figure 4 presents the spatial trajectories of the four mobile sensor/actuator pairs. It visually verifies that

all mobile nodes are strictly confined within their prescribed safety subdomains $W_{ijs}$ (dashed boxes), inherently guaranteeing the avoidance of physical collisions.

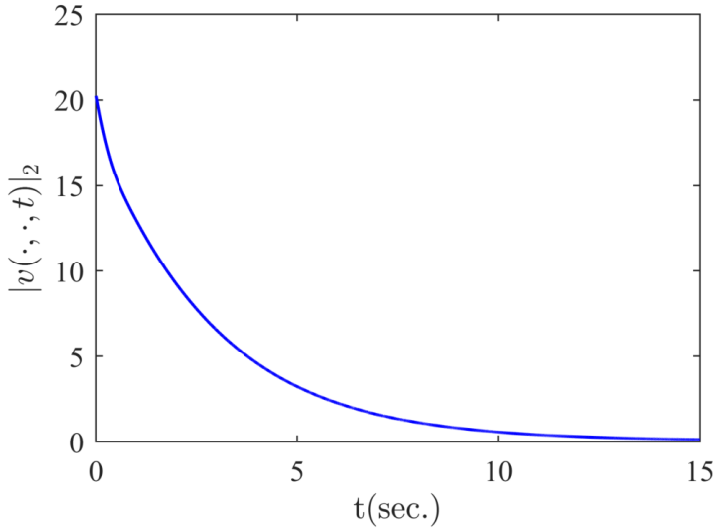


**Figure 2.** Closed-loop response of (2.1)–(2.3): Trajectory of $|v(\cdot,\cdot,t)|_2$.

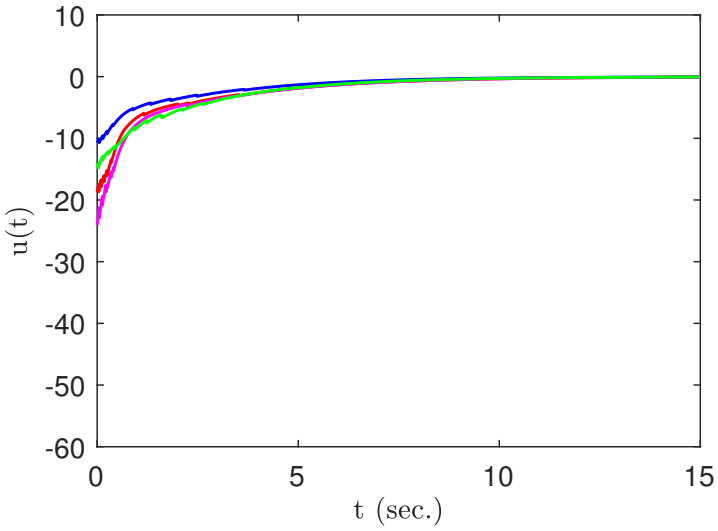


**Figure 3.** Control inputs of the closed-loop system. The solid red line shows $u_{11}(t)$, the blue line shows $u_{12}(t)$, the purple line shows $u_{21}(t)$, and the green line shows $u_{22}(t)$.

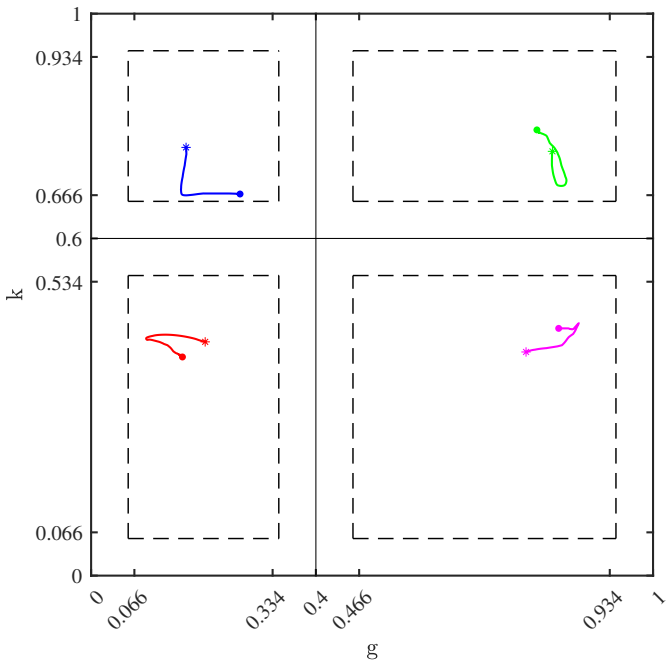


**Figure 4.** Trajectories of four mobile collocated sensor/actuator pairs. The red, blue, purple, and green lines show the movement trajectories of $(g^a_{11}(t), k^a_{11}(t))$, $(g^a_{12}(t), k^a_{12}(t))$, $(g^a_{21}(t), k^a_{21}(t))$, and $(g^a_{22}(t), k^a_{22}(t))$, respectively. The symbols $*$ and $\bullet$ indicate the starting and ending positions.

In this section, through the numerical simulations, the method's superior performance in dynamic response is verified. In the future, we will build an experimental platform to bridge the simulation-to-implementation gap by quantifying real-world factors such as communication latency and mechanical hysteresis, where the following kinematic model of each mobile sensor/actuator pair will be considered:

$$\dot{g}^a(t) = v\cos\varphi,\ \dot{k}^a(t) = v\sin\varphi,\ \dot{\varphi} = \omega$$

in which $v$ and $\omega$ indicate the linear velocity and angular velocity, respectively, and they are the vehicle control inputs. When the kinematic model is considered, the trajectory tracking control issue of mobile vehicles needs to be resolved, which is very meaningful and valuable.

## 5. Conclusions

This paper has presented a comprehensive investigation into the Lyapunov-based stabilization issue of spatial 2-D linear parabolic DPSs with moving sensor/actuator pairs. The study makes three fundamental contributions to the field of DPS control. First, we conduct a theoretical analysis of system well-posedness, examining both the open-loop and closed-loop systems through functional analysis and semigroup theory. This analysis establishes crucial properties of existence, uniqueness, and continuity that form the mathematical foundation for subsequent control design. Second, we develop an integrated design methodology that simultaneously addresses control synthesis

and sensor/actuator guidance. The proposed approach combines Lyapunov stability theory with sensor/actuator placement strategies, creating a unified framework that coordinates control action with spatial reconfiguration. The control design employs a Lyapunov control technique adapted for the mobile sensor/actuator scenario, and the guidance scheme incorporates real-time performance metrics to determine optimal positioning. Third, the theoretical developments are validated through numerical simulations. The practical implications of this work extend to various engineering applications requiring spatial control, including thermal regulation in advanced manufacturing, contaminant mitigation in environmental systems, and distributed parameter control in chemical processes. Future research directions include extension to spatial 2-D nonlinear PDE systems, the incorporation of sensor/actuator dynamic constraints, and the development of event-triggered implementation for reduced the computational burden.

## Author contributions

Xiao-Wei Zhang: Writing – original draft, conceptualization, methodology, writing – review and editing, software; Xiang-Jie Pu: Writing – original draft, formal analysis, software; Xiaoli Li: Writing – review and editing, methodology, validation; Zi-Peng Wang: Visualization, supervision, data curation. All authors have read and approved the final version of the manuscript.

## Use of Generative-AI tools declaration

The authors declare they have not used Artificial Intelligence (AI) tools in the creation of this article.

## Acknowledgments

This work was supported in part by the National Natural Science Foundation of China under Grants 62573009 and 62373012, in part by the Postdoctoral Fellowship Program of China Postdoctoral Science Foundation under Grant GZC20251205, in part by the China Postdoctoral Science Foundation under Grant 2024M760172, in part by the Beijing Postdoctoral Science Foundation under Grant 2025-ZZ-35, and in part by the Fundamental Research Funds for Beijing Municipal Universities under Grant 312000546325001.

## Conflict of interest

Prof. Zi-Peng Wang is an editorial board member for AIMS Mathematics and was not involved in the editorial review and the decision to publish this article.

The authors declare no conflicts of interest.

## References

1. W. Kang, X. N. Wang, B. Z. Guo, Observer-based fuzzy quantized control for a stochastic third-order parabolic PDE system, *IEEE Trans. Syst. Man Cybern. Syst.*, **53** (2023), 485–494. https://doi.org/10.1109/TSMC.2022.3184077

2. Z. Liu, Z. Zhao, C. K. Ahn, Boundary constrained control of flexible string systems subject to disturbances, *IEEE Trans. Circuits Syst. II Express Briefs*, **67** (2020), 112–116. https://doi.org/10.1109/TCSII.2019.2901283
3. J. F. Zhang, J. W. Wang, H. K. Lam, H. X. Li, Boundary output tracking of nonlinear parabolic differential systems via fuzzy PID control, *IEEE Trans. Fuzzy Syst.*, **32** (2024), 6863–6877. https://doi.org/10.1109/TFUZZ.2024.3432554
4. H. Wei, X. Cui, Y. Zhang, J. Zhang, $H_\infty$ deployment of nonlinear multi-agent systems with Markov switching topologies over a finite-time interval based on T–S fuzzy PDE control, *AIMS Math.*, **9** (2024), 4076–4097. https://doi.org/10.3934/math.2024199
5. Z. Zhao, X. He, Z. Ren, G. Wen, Boundary adaptive robust control of a flexible riser system with input nonlinearities, *IEEE Trans. Syst. Man Cybern. Syst.*, **49** (2019), 1971–1980. https://doi.org/10.1109/TSMC.2018.2882734
6. X. Song, J. Man, S. Song, C. K. Ahn, Finite-time fault estimation and tolerant control for nonlinear interconnected distributed parameter systems with Markovian switching channels, *IEEE Trans. Circuits Syst. I Reg. Pap.*, **69** (2022), 1347–1359. https://doi.org/10.1109/TCSI.2021.3129372
7. M. Krstic, A. Smyshlyaev, *Boundary control of PDEs: A course on backstepping designs*, Philadelphia: SIAM, 2008. https://doi.org/10.1137/1.9780898718607
8. A. Smyshlyaev, M. Krstic, *Adaptive control of parabolic PDEs*, Princeton: Princeton University Press, 2010. https://doi.org/10.1515/9781400835362
9. L. Su, W. Guo, J. M. Wang, M. Krstic, Boundary stabilization of wave equation with velocity recirculation, *IEEE Trans. Autom. Control*, **62** (2017), 4760–4767. https://doi.org/10.1109/TAC.2017.2688128
10. J. Deutscher, A backstepping approach to the output regulation of boundary controlled parabolic PDEs, *Automatica*, **57** (2015), 56–64. https://doi.org/10.1016/j.automatica.2015.04.008
11. B. Z. Guo, R. X. Zhao, Output regulation for a heat equation with unknown exosystem, *Automatica*, **138** (2022), 110159. https://doi.org/10.1016/j.automatica.2022.110159
12. B. Z. Guo, H. C. Zhou, The active disturbance rejection control to stabilization for multi-dimensional wave equation with boundary control matched disturbance, *IEEE Trans. Autom. Control*, **60** (2015), 143–157. https://doi.org/10.1109/TAC.2014.2335511
13. R. Katz, E. Fridman, Delayed finite-dimensional observer-based control of 1-D parabolic PDEs, *Automatica*, **123** (2021), 109364. https://doi.org/10.1016/j.automatica.2020.109364
14. X. Lu, W. Zou, M. Huang, A novel spatiotemporal LS-SVM method for complex distributed parameter systems with applications to curing thermal process, *IEEE Trans. Ind. Informat.*, **12** (2016), 1156–1165. https://doi.org/10.1109/TII.2016.2557805
15. X. Lu, W. Zou, M. Huang, An adaptive modeling method for time-varying distributed parameter processes with curing process applications, *Nonlinear Dyn.*, **82** (2015), 865–876. https://doi.org/10.1007/s11071-015-2201-3
16. W. He, X. He, M. Zou, H. Li, PDE model-based boundary control design for a flexible robotic manipulator with input backlash, *IEEE Trans. Control Syst. Technol.*, **27** (2019), 790–797. https://doi.org/10.1109/TCST.2017.2780055

17. X. Song, R. Zhang, S. Song, Y. Zhang, Fuzzy adaptive-event-triggered control for semi-linear parabolic PDE systems with stochastic actuator failures, *Appl. Math. Comput.*, **426** (2022), 127127. https://doi.org/10.1016/j.amc.2022.127127

18. J. W. Wang, J. F. Zhang, H. N. Wu, Boundary fuzzy output tracking control of nonlinear parabolic infinite-dimensional dynamic systems: Application to cooling process in hot strip mills, *IEEE Trans. Fuzzy Syst.*, **31** (2023), 1460–1473. https://doi.org/10.1109/TFUZZ.2022.3203524

19. J. W. Wang, Y. H. Wei, P. Shi, Spatiotemporal adaptive fuzzy control for state profile tracking of nonlinear infinite-dimensional systems on a hypercube, *IEEE Trans. Fuzzy Syst.*, **32** (2024), 683–696. https://doi.org/10.1109/TFUZZ.2023.3307619

20. X. Dai, Y. Wang, S. Tian, Y. Chen, Z. Zhao, Fuzzy iterative learning control for nonlinear parabolic distributed parameter systems, *Fuzzy Sets Syst.*, **521** (2025), 109603. https://doi.org/10.1016/j.fss.2025.109603

21. J. F. Zhang, J. W. Wang, H. K. Lam, H. X. Li, Boundary output tracking of nonlinear parabolic differential systems via fuzzy PID control, *IEEE Trans. Fuzzy Syst.*, **32** (2024), 6863–6877. https://doi.org/10.1109/TFUZZ.2024.3432554

22. X. Dai, H. Zuo, F. Deng, Mean square finite-time stability and stabilization of impulsive stochastic distributed parameter systems, *IEEE Trans. Syst. Man Cybern. Syst.*, **55** (2025), 4064–4075. https://doi.org/10.1109/TSMC.2025.3547949

23. X. Dai, Y. Xu, F. Deng, Mean-square finite and prescribed-time stability for nonlinear stochastic parabolic distributed parameter systems, *Commun. Nonlinear Sci. Numer. Simul.*, **145** (2025), 108688. https://doi.org/10.1016/j.cnsns.2025.108688

24. F. Zeng, B. Ayalew, Estimation and coordinated control for distributed parameter processes with a moving radiant actuator, *J. Process Control*, **20** (2010), 743–753. https://doi.org/10.1016/j.jprocont.2010.04.005

25. Y. H. Wei, J. W. Wang, Q. Zhang, Reinforcement learning-based optimal formation control of multiple robotic rollers in cooperative rolling compaction, *Robotics Auton. Syst.*, **189** (2025), 104947. https://doi.org/10.1016/j.robot.2025.104947

26. M. A. Demetriou, Guidance of a moving collocated actuator/sensor for improved control of distributed parameter systems, In: *2008 47th IEEE conference on decision and control*, 2008. https://doi.org/10.1109/CDC.2008.4739040

27. W. Mu, B. Cui, W. Li, Z. Jiang, Improving control and estimation for distributed parameter systems utilizing mobile actuator-sensor network, *ISA Trans.*, **53** (2014), 1087–1095. https://doi.org/10.1016/j.isatra.2014.05.004

28. S. Cheng, D. A. Paley, Optimal control of a 1D diffusion process with a team of mobile actuators under jointly optimal guidance, In: *2020 American control conference*, 2020. https://doi.org/10.23919/acc45564.2020.9147830

29. H. Fu, B. Cui, B. Zhuang, J. Zhang, Anti-collision and obstacle avoidance of mobile sensor-plus-actuator networks over distributed parameter systems with time-varying delay, *Int. J. Control Autom. Syst.*, **19** (2021), 2373–2384. https://doi.org/10.1007/s12555-020-0317-9

30. Y. Liu, J. W. Wang, Z. Wu, Z. Ren, S. Xie, Robust $H_\infty$ control for semilinear parabolic distributed parameter systems with external disturbances via mobile actuators and sensors, *IEEE Trans. Cybern.*, **53** (2023), 4880–4893. https://doi.org/10.1109/TCYB.2022.3150171

31. W. Kang, E. Fridman, C. X. Liu, Stabilization by switching of parabolic PDEs with spatially scheduled actuators and sensors, *Automatica*, **147** (2023), 110668. https://doi.org/10.1016/j.automatica.2022.110668

32. X. W. Zhang, Q. Zhou, H. N. Wu, J. L. Wang, Z. P. Wang, Lyapunov-based stabilization mobile control design of linear parabolic PDE systems, *Chaos Soliton Fract.*, **175** (2023), 114002. https://doi.org/10.1016/j.chaos.2023.114002

33. X. W. Zhang, H. N. Wu, $H_\infty$ control design for non-linear distributed parameter systems with mobile actuators and sensors, *IET Control Theory Appl.*, **13** (2019), 2228–2238. https://doi.org/10.1049/iet-cta.2019.0092

34. H. N. Wu, X. W. Zhang, Static output feedback stabilization for a linear parabolic PDE system with time-varying delay via mobile collocated actuator/sensor pairs, *Automatica*, **117** (2020), 108993. https://doi.org/10.1016/j.automatica.2020.108993

35. X. W. Zhang, H. N. Wu, Fuzzy stabilization design for semilinear parabolic PDE systems with mobile actuators and sensors, *IEEE Trans. Fuzzy Syst.*, **28** (2020), 474–486. https://doi.org/10.1109/TFUZZ.2019.2908139

36. X. W. Zhang, H. N. Wu, Fuzzy control design of nonlinear time-delay parabolic PDE systems under mobile collocated actuators and sensors, *IEEE Trans. Cybern.*, **52** (2022), 3947–3956. https://doi.org/10.1109/TCYB.2020.3020087

37. X. W. Zhang, H. N. Wu, J. L. Wang, Y. Ji, N. Rong, Observer-based boundary fuzzy control design of nonlinear parabolic PDE systems using mobile sensors, *IEEE Trans. Fuzzy Syst.*, **31** (2023), 3485–3494. https://doi.org/10.1109/TFUZZ.2023.3260102

38. S. Cheng, D. A. Paley, Cooperative estimation and control of a diffusion-based spatiotemporal process using mobile sensors and actuators, *Auton. Robots*, **47** (2023), 715–731. https://doi.org/10.1007/s10514-023-10105-9

39. N. A. Gatsonis, M. A. Demetriou, T. Egorova, Real-time prediction of gas contaminant concentration from a ground intruder using a UAV, In: *2015 IEEE international symposium on technologies for homeland security*, 2015. https://doi.org/10.1109/THS.2015.7225276

40. M. A. Demetriou, Controlling 2D PDEs using mobile collocated actuators-sensors and their simultaneous guidance constrained over path-dependent reachability regions, In: *2021 American control conference*, 2021. https://doi.org/10.23919/acc50511.2021.9482892

41. Y. Q. Chen, Z. Wang, J. Liang, Actuation scheduling in mobile actuator networks for spatial-temporal feedback control of a diffusion process with dynamic obstacle avoidance, In: *IEEE international conference mechatronics and automation*, 2005. https://doi.org/10.1109/ICMA.2005.1626644

42. Y. Q. Chen, Z. Wang, J. Liang, Optimal dynamic actuator location in distributed feedback control of a diffusion process, In: *Proceedings of the 44th IEEE conference on decision and control*, 2005. https://doi.org/10.1109/cdc.2005.1583065

43. S. Cheng, D. A. Paley, Optimal control of a 2D diffusion-advection process with a team of mobile actuators under jointly optimal guidance, *Automatica*, **133** (2021), 109866. https://doi.org/10.1016/j.automatica.2021.109866
44. S. Cheng, D. A. Paley, Optimal guidance and estimation of a 2D diffusion-advection process by a team of mobile sensors, *Automatica*, **137** (2022), 110112. https://doi.org/10.1016/j.automatica.2021.110112
45. M. A. Demetriou, Guidance of mobile actuator-plus-sensor networks for improved control and estimation of distributed parameter systems, *IEEE Trans. Autom. Control*, **55** (2010), 1570–1584. https://doi.org/10.1109/tac.2010.2042229
46. M. A. Demetriou, Adaptive control of 2-D PDEs using mobile collocated actuator/sensor pairs with augmented vehicle dynamics, *IEEE Trans. Autom. Control*, **57** (2012), 2979–2993. https://doi.org/10.1109/tac.2012.2196402
47. J. W. Wang, Y. Q. Liu, C. Y. Sun, Observer-based dynamic local piecewise control of a linear parabolic PDE using non-collocated local piecewise observation, *IET Control Theory Appl.*, **12** (2018), 346–358. https://doi.org/10.1049/iet-cta.2017.0797
48. R. F. Curtain, H. Zwart, *An introduction to infinite-dimensional linear systems theory*, New York: Springer, 1995. https://doi.org/10.1007/978-1-4612-4224-6
49. J. W. Wang, J. M. Wang, Dynamic compensator design of linear parabolic MIMO PDEs in $N$-dimensional spatial domain, *IEEE Trans. Autom. Control*, **66** (2021), 1399–1406. https://doi.org/10.1109/TAC.2020.2994165
50. A. Pazy, *Semigroups of linear operators and applications to partial differential equations*, New York: Springer, 1983. https://doi.org/10.1007/978-1-4612-5561-1
51. H. Peng, Q. Zhu, Finite-time stability and stabilization of highly nonlinear stochastic systems via the noise control, *IEEE Trans. Autom. Control*, 2026, in press. https://doi.org/10.1109/TAC.2026.3660601
52. Q. Zhu, Event-triggered sampling problem for exponential stability of stochastic nonlinear delay systems driven by Lévy processes, *IEEE Trans. Autom. Control*, **70** (2025), 1176–1183. https://doi.org/10.1109/tac.2024.3448128
53. H. Xu, Q. Zhu, Stability of discrete-time impulsive stochastic systems with hybrid non-deterministic delays, *IEEE Trans. Autom. Control*, 2026, in press. https://doi.org/10.1109/TAC.2026.3666702
54. J. W. Wang, F. Wang, H. N. Wu, Z. Y. Liu, Safe RL-based adaptive cooperative game control of wing deformation and flight state tracking for morphing hypersonic vehicles, *IEEE Trans. Aerosp. Electron. Syst.*, **61** (2025), 10826–10838. https://doi.org/10.1109/taes.2025.3560610



AIMS Press

© 2026 the Author(s), licensee AIMS Press. This is an open access article distributed under the terms of the Creative Commons Attribution License (https://creativecommons.org/licenses/by/4.0)